Kinetic modeling of plasma response to RMPs for a tokamak in full toroidal geometry

C. G. Albert[1,2], M. F. Heyn[1], S. V. Kasilov[1,3], W. Kernbichler[1], the EUROfusion MST1 Team*

[1] *Fusion@ÖAW, ITPcp, TU Graz, Petersgasse 16, 8010 Graz, Austria*

[2] *Max-Planck-Institut für Plasmaphysik, Boltzmannstraße 2, 85748 Garching, Germany*

[3] *Institute of Plasma Physics, NSC KIPT, Akademicheskaya Str. 1, 61108 Kharkov, Ukraine*

* *See the author list "H. Meyer et al 2017 Nucl. Fusion 57 102014"*

Introduction

Kinetic modeling has recently been presented [1, 2] for predicting the penetration of resonant magnetic perturbations (RMPs) into a tokamak plasma. A substantial reduction in computation time would be possible if part of the full kinetic problem could be solved by a less complex model. One candidate for such a method would be the reduction to ideal magnetohydrodynamics (MHD) that is expected to be valid away from resonant surfaces. Before this can be realized, it is necessary to cross-validate both models in their common range of applicability. Here the comparison between kinetic and MHD modeling of the plasma pressure response to a test field representing the non-resonant part of a resonant magnetic perturbation (RMP) is presented as well as a computation for the actual ELM mitigation coils in ASDEX Upgrade.

Plasma models

A linear ideal MHD model has been chosen in such a way that it can be used as a drop-in replacement for the gyrokinetic equation solver presented in [2] and is defined on the same field-aligned triangular grid in the poloidal plane in cylindrical coordinates (R,φ,Z). Based on an equilibrium $c\nabla p_0 = \mathbf{j}_0 \times \mathbf{B}_0$ for pressure p_0, current density $\mathbf{j}_0$ and magnetic field $\mathbf{B}_0$, toroidal harmonics p_n, $\mathbf{j}_n$ and $\mathbf{B}_n$ are introduced for a linear order perturbation. Perturbed quantities fulfill the linearized force balance equation and current divergence-freeness,

$$c(\nabla p_n + \mathrm{i} n p_n \nabla\varphi) = \mathbf{j}_0 \times \mathbf{B}_n - \mathbf{j}_n \times \mathbf{B}_0, \tag{1}$$

$$\nabla \cdot \mathbf{j}_n^{\mathrm{pol}} + \mathrm{i} n j_n^{\varphi} = 0. \tag{2}$$

From those equations p_n and $\mathbf{j}_n$ can be computed for a given $\mathbf{B}_n$, corresponding to half an iteration step in [2]. Projecting Eq. (1) towards $\mathbf{B}_0$ and inserting the unperturbed force balance, p_n is computed first by solving the resulting magnetic differential equation in the poloidal plane along each edge loop on a field-aligned mesh in a finite difference scheme. Eq. (2) has the form of a conservation law for $\mathbf{j}_n^{\mathrm{pol}}$ that is solved on a face loop between two edge loops by a finite volume scheme. There the toroidal current perturbation j_n^{φ} is expressed via $\mathbf{j}_n^{\mathrm{pol}}$ and the already known p_n by projection of Eq. (1) to element edges in the poloidal plane.

For kinetic computations a linear δf Monte Carlo model using a geometric integrator [2, 3, 4] is applied in its "collisionless" form, computing orbits for only one bounce period with a Krook collision operator. Such a simplification of the collision model can be done in most plasma

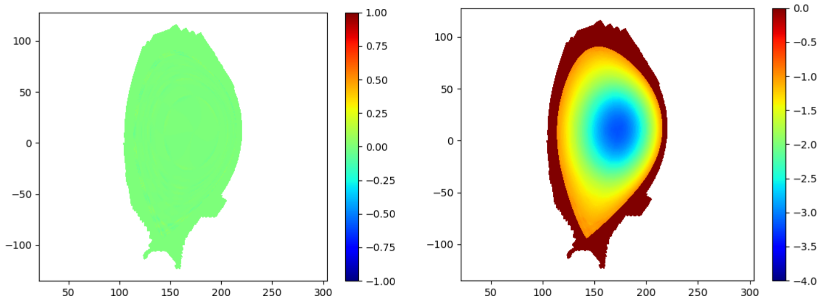

Figure 1: Ideal MHD response pressure p_n to non-resonant field. *Left:* real part, *right:* imaginary part.

volume except for the narrow resonant layers around rational flux surfaces where the parallel wavelength of the perturbation field strongly increases and becomes comparable or larger than the mean free path. Both, parallel $p_{\|}$ and perpendicular component $p_{\perp}$ of the Chew-Goldberger-Low pressure tensor are computed directly from the time-averaged test particle distribution.

Results

Computations have been performed in the typical parameter range of ASDEX Upgrade (see [5]) and a perturbation with toroidal harmonic $n = 2$. All parameter profiles were linear functions of poloidal flux with central density $5 \cdot 10^{13}$ cm^{-3}, temperature of 3 keV and electrostatic potential of 2 kV. Results are shown as contour plots of $n = 2$ toroidal mode Fourier amplitudes for the single-iteration plasma pressure response p_n, $p_{\|n}$, $p_{\perp n}$ in arbitrary units and lengths in cm.

Figs. 1-4 show the response to an artificial fully non-resonant perturbation field defined by $B^{\psi} \propto R^{-2}$. Parallel pressures from kinetic computations for both, electrons and ions in Fig. 2 agree well to the MHD scalar pressure in Fig. 1. However, the perpendicular kinetic pressure response in Fig. 3 shows structures of different amplitude and phase. Increasing the equilibrium radial electric field E_r by factor 10 (Fig. 4) restores an ideal MHD-like response for electrons, but not for ions, where the banana-orbit-like shape of the response becomes even more apparent.

It has been shown [5] that for a reactor-relevant low-collisionality shot in ASDEX Upgrade non-ambipolar transport and neoclassical toroidal viscosity (NTV) for ions was mainly governed by "collisionless" resonant transport regimes [6]. Such regimes are divided into the superbanana plateau regime, occuring for a radial electric field E_r close to zero, and the remaining resonant plateau regime due to drift-orbit resonances that strongly affect ion NTV in a wide range of values for E_r [7]. The resonant plateau is much weaker for electrons due to their higher bounce and collision frequencies. An increase in E_r moves the superbanana resonance to the high energy tail of the distribution function thus making it irrelevant, while keeping and even enhancing a resonant plateau for ions.

Fig. 5 shows the real part of the pressure response to a resonant magnetic perturbation in the ASDEX Upgrade tokamak with ELM mitigation coils for MHD and kinetic model. Here the resonant structure of the parallel pressure response $p_{\|}$ agrees well between ideal MHD and electron kinetics, where the latter is slightly damped due to collisions. However, the resonant response of $p_{\|}$ for ions, having a substantially larger orbit width, shows visible differences in the distribution of structures around resonant surfaces. Results for the imaginary part are similar and as in the non-resonant case $p_{\perp}$ is affected more strongly, which is not plotted here.

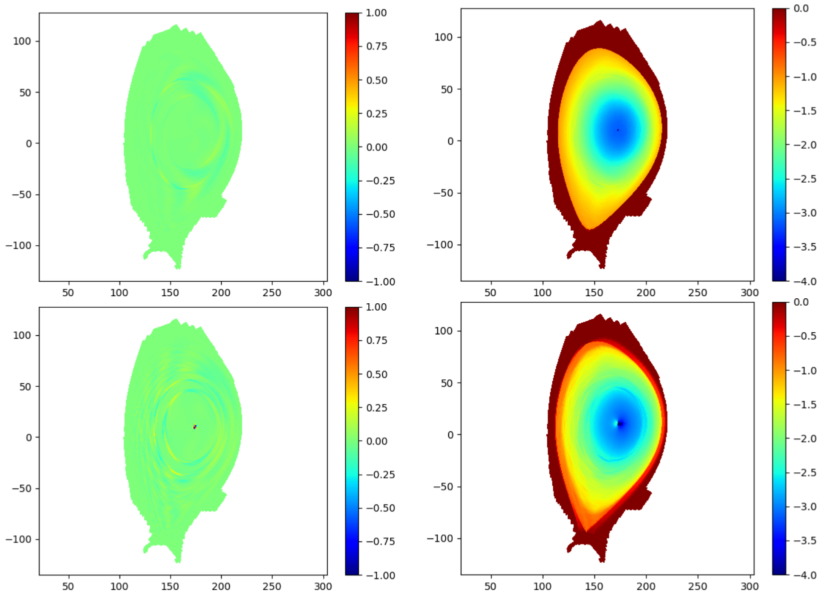

Figure 2: Kinetic parallel response pressure $p_{\parallel n}$ to non-resonant field. *Left:* real part, *right:* imaginary part, *top:* electrons, *bottom:* ions.

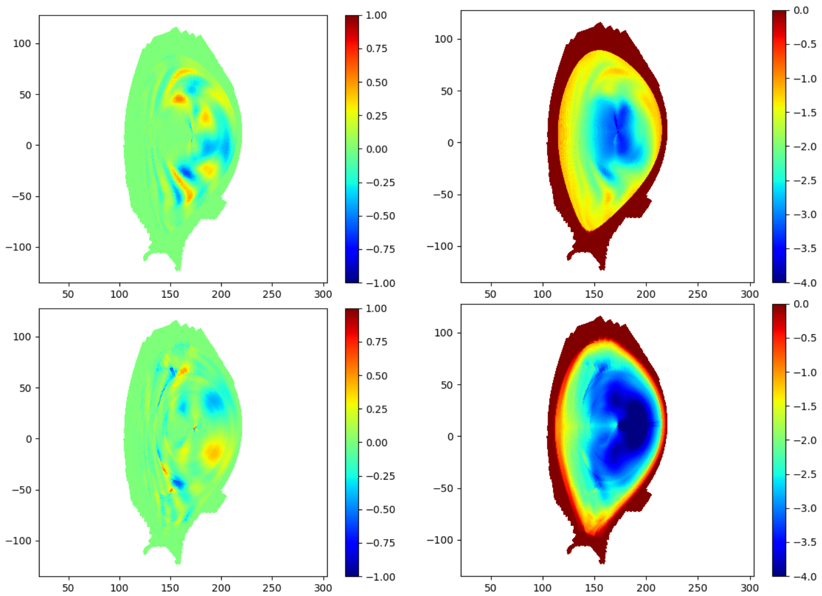

Figure 3: Kinetic perpendicular response pressure $p_{\perp n}$ to non-resonant field. *Left:* real part, *right:* imaginary part, *top:* electrons, *bottom:* ions, structures visible for both.

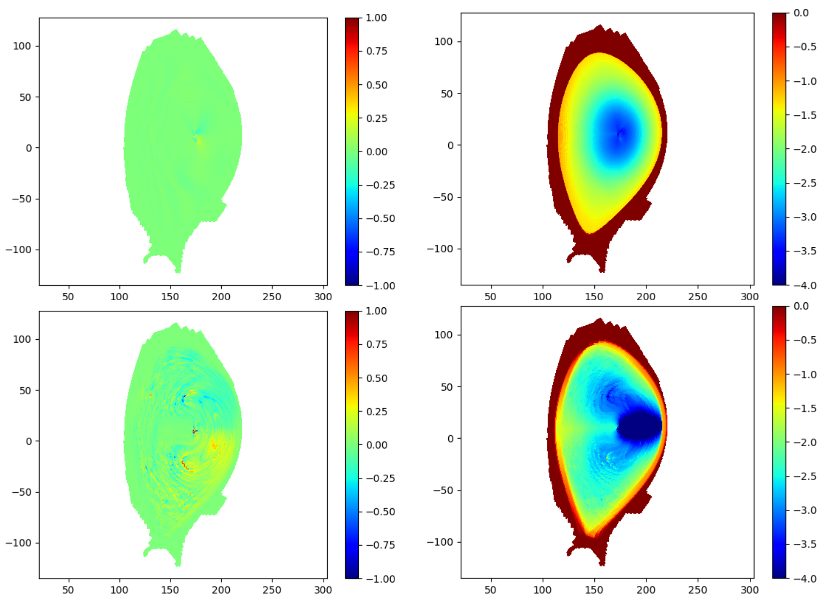

Figure 4: Kinetic perpendicular response pressure $p_{\perp n}$ to non-resonant field, radial electric field increased by factor 10. *Left:* real part, *right:* imaginary part, *top:* electrons, *bottom:* ions. Orbit-like structures disappear for electrons but remain for ions.

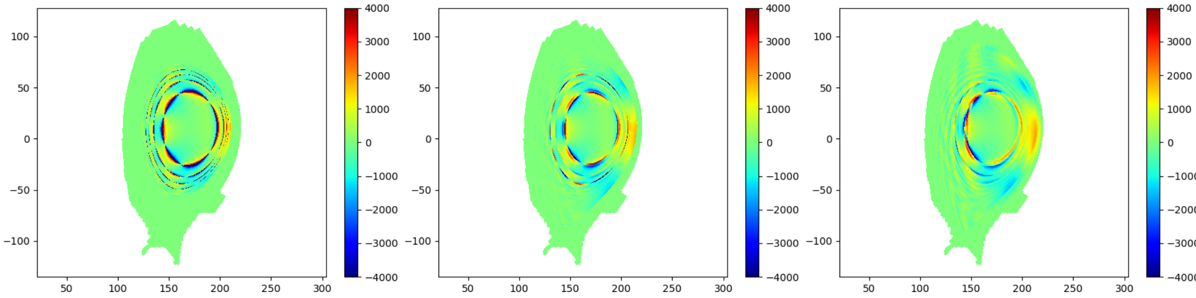

Figure 5: Real part of response pressure to resonant field of ELM mitigation coils in ASDEX Upgrade. *Left:* MHD, *middle:* kinetic electron $p_\parallel$ *right:* kinetic ion $p_\parallel$ with visible structure.

Conclusion

A comparison between the pressure response due to external magnetic perturbations has been performed between low-collisional kinetics and ideal MHD. The presented results show that the parallel part of the kinetic pressure response due to a non-resonant perturbation agrees well with the ideal MHD pressure response. The perpendicular pressure response, which determines perturbation of diamagnetic currents, is however affected by kinetic effects that are interpreted to result from orbital resonances. This is supported by the disappearance of the effect for electrons by increasing the radial electric field, thereby removing the superbanana resonance. Structures specific to the kinetic model are also visible in the response to a resonant magnetic perturbation and in contrast to the non-resonant case appear also in the parallel ion pressure. This is most likely linked to the larger orbit width of ions. Further investigations on a fully iterated solution are required to verify the differences between ideal MHD and kinetic plasma response.

Acknowledgements

This work has been carried out within the framework of the EUROfusion Consortium and has received funding from the Euratom research and training programme 2014-2018 under grant agreement No 633053. The views and opinions expressed herein do not necessarily reflect those of the European Commission. The authors gratefully acknowledge support from NAWI Graz, from the OeAD under the WTZ grant agreement with Ukraine No UA 04/2017 and funding from the Helmholtz Association within the research project "Reduced Complexity Models".

References

[1] M. Heyn *et al.*, Nucl. Fusion **54**, 064005 (2014).
[2] C. Albert *et al.*, J. Phys. Conf. Series **775**, 012001 (2016).
[3] A. M. Runov, S. V. Kasilov, and P. Helander, J. Comput. Phys. **300**, 605 (2015).
[4] S. V. Kasilov, A. M. Runov, and W. Kernbichler, Comp. Phys. Comm. **207**, 282 (2016).
[5] A. Martitsch *et al.*, Plasma Phys. Contr. Fusion **58**, 074007 (2016).
[6] K. Shaing, K. Ida, and S. Sabbagh, Nuclear Fusion **55**, 125001 (2015).
[7] C. Albert *et al.*, Phys. Plasmas **23**, 082515 (2016).